High Temperature. Vol. 43, No. 5, 2005, pp. 733–745. Translated from Teplofizika Vysokikh Temperatur, Vol. 43, No. 5, 2005, pp. 732–744.
Original Russian Text Copyright © 2005 by V. A. Bashkin, I. V. Egorov, and V. V. Pafnut'ev.

HEAT AND MASS TRANSFER AND PHYSICAL GASDYNAMICS

Aerodynamic Heating of a Thin Sharp-Nose Circular Cone in Supersonic Flow

V. A. Bashkin, I. V. Egorov, and V. V. Pafnut'ev

N.E. Zhukovskii Central Institute of Aerohydrodynamics (TsAGI), Zhukovskii, Moscow oblast, 140160 Russia

Received April 20, 2004

Abstract—The assumption of flow symmetry is made to investigate a supersonic flow ($M_\infty = 5$) past a thin circular cone with a half-angle $\theta_c = 4°$ and an isothermal surface ($T_{w0} = 0.5$) by way of numerical integration of unsteady-state three-dimensional Navier–Stokes and Reynolds equations. The calculations are performed in a discrete range of variation of the Reynolds number ($10^4 \le Re \le 10^8$) and angle of attack ($0° \le \alpha \le 15°$). The effect of the determining parameters of the problem on the structure of flow field and on aerodynamic heating of the body surface subjected to flow is demonstrated.

INTRODUCTION

Sharp-nose circular cones are often used as elements of flying vehicles; therefore, the investigation of flow past these bodies is of scientific and applied interest. In view of this, the flow past conical bodies has been studied theoretically and experimentally in a fairly wide range of variation of the determining parameters of the problem. The results of these studies are generalized in a number of monographs, for example, in monographs [1, 2] devoted to supersonic and hypersonic flows of gas past sharp-nose conical bodies.

The experimental investigations cover two ranges with respect to the Mach number. The first range includes transonic and low supersonic velocities ($0.6 < M_\infty < 3$), and the second range – hypersonic velocities at which the rarefied gas effects show up ($M_\infty > 10$). A typical example of investigations of the first type is provided by studies [3, 4], and of those of the second type – by study [5]. Note that the Mach numbers in the first range were extensively employed in aviation technologies, and those in the second range – in space technologies. Experimental investigations of sharp-nose conical bodies at high values of the Mach number were performed as well; however, preference was given to the study of blunt conical bodies under conditions of aerodynamic heating.

According to the results of investigations performed at high values of the Reynolds number, the structure of flow field in the vicinity of a thin circular cone with a half-angle θ_c located at an angle of attack α in supersonic flow is largely defined by the angle of attack.

At low angles of attack ($\alpha/\theta_c \le 0.8$), the flow past a cone is non-separation and symmetric. In so doing, the line of spreading is located in the plane of symmetry on the windward side of the cone, and the line of runoff – on the leeward side. The pressure assumes extreme values on these lines in the cone cross section, namely, the maximal value on the spreading line and the minimal value on the runoff line; consequently, the transverse flow in the boundary layer is directed from the spreading line to runoff line.

A transverse separation of the boundary layer is observed on the leeward side of the cone at moderate and high values of the angle of attack ($0.8 < \alpha/\theta_c$). According to the experimental data, a symmetric separation of flow is observed for the number $M_\infty = 1.8$ [4] at angles of attack $\alpha/\theta_c \le 3.2$, which causes the symmetry of flow past the cone, and an asymmetric separation of flow is observed at angles of attack $\alpha/\theta_c > 3.2$, which causes the asymmetry of gas flow in the vicinity of the cone and the emergence of a lateral force. In so doing, the limiting value of the angle of attack increases with the Mach number.

Theoretical investigations of supersonic flow past sharp-nose cones involved an extensive use of the

0018-151X/05/4305-0733 © 2005 Russian Academy of Sciences and Springer Science + Business Media, Inc.

classical (asymptotic) formulation of the problem, in which nonviscous flow plus noninteracting boundary layer were treated.

Within the classical formulation of the problem, a nonviscous flow in the vicinity of a sharp circular cone is conical in the case of small and moderate angles of attack, and the solution of equations of three-dimensional boundary layer in the case of conical external flow is self-similar under certain conditions and reduces to integrating the set of parabolic two-dimensional equations. The flow of gas in turbulent boundary layer is non-self-similar under any conditions and retains a significantly three-dimensional pattern.

In the case of asymptotic approach, only the flow fields and local aerodynamic characteristics in the region of non-separation flow past a body are determined. As is demonstrated by the results of theoretical and experimental investigations, local "peaks" of heat flux arise in separation flow regions, which have a significant effect on aerodynamic heating of the surface subjected to flow and are of much interest from the standpoint of applied problems.

In view of this, it is necessary to solve the problem using complete equations of viscous gas dynamics.

A number of theoretical investigations of supersonic flow past conical bodies were performed assuming the conical pattern of viscous gas flow, owing to which the numerical integration of unsteady-state three-dimensional Navier–Stokes or Reynolds equations reduces to solving an unsteady-state two-dimensional problem (see, for example, [6]). The results of calculations using this approximate approach agree quite well with the respective experimental data. The studies devoted to numerical simulation of supersonic flow past sharp-nose cones using complete equations of viscous gas dynamics are relatively few and, as a rule, deal with the evaluation of numerical algorithm.

At present, the aviation and space technologies involve ever higher supersonic velocities, and the need arises for studying supersonic flows past sharp-nose thin cones at high values of the Mach number at the angle of attack using equations of viscous gas dynamics.

Numerous different approaches to numerical solution of Navier–Stokes and Reynolds equations have been developed within the framework of computational aerodynamics. These approaches include the method based on the implicit finite-difference scheme of Beam and Warming [7] and its further modification [8, 9].

The use of implicit difference schemes with subsequent linearization and solution of the set of finite-difference equations by the Newton method [10] may be regarded as the most complete from the mathematical standpoint. This approach was developed for numerical integration of unsteady-state two-dimensional Navier–Stokes equations [11] and Reynolds equations [12] in the Boussinesq assumption of Reynolds stresses using a two-parameter differential model of turbulence [13] and realized in a software package for personal computers (PC). It was further used to solve a number of supersonic problems of external and internal aerodynamics such as those for circular cylinder, sphere, and plane and axisymmetric channels [14]. The development of PC as regards the increase in their speed and memory made it possible to generalize this approach to the simulation of three-dimensional supersonic flows using unsteady-state three-dimensional equations of viscous gas dynamics [15, 16]. The procedure of numerical simulation using Navier–Stokes equations is described in [15] and verified by comparing the calculation results ($M_\infty = 10.4$, $\theta_c = 15°$, $0 \le \alpha/\theta_c \le 1.2$) with experimental data [17]. The procedure of numerical simulation using Reynolds equations is described in [16], and the calculation results and experimental data ($M_\infty = 4$, $\theta_c = 4°$, $0 \le \alpha/\theta_c \le 2$) are compared with respect to the integral characteristics of a sharp cone. In both latter studies, the calculations were performed on the assumption of flow symmetry, and good quantitative and qualitative agreement was observed between the theoretical and experimental data. This fact enables one to use this approach to investigate a supersonic flow of viscous gas past sharp-nose conical bodies.

We have performed a numerical investigation of aerodynamic heating of a thin sharp-nose circular cone in a supersonic flow of viscous perfect gas at high values of the Reynolds number in some range of values of the attack angle. Because the special features of heat transfer on the cone surface subjected to flow are defined by the structure of the flow field, the study of the latter as a function of the angle of attack and Reynolds number is likewise given considerable attention. In the first section of this paper, the formulation of the problem and the calculation conditions are described briefly; the second section deals with the effect of the angle of attack and Reynolds number on the structure of flow field; in the third section, special

features of heat transfer on the surface of a cone subjected to flow are analyzed.

FORMULATION OF THE PROBLEM AND CONDITIONS OF CALCULATION

Numerical integration of Navier–Stokes and Reynolds equations by the procedure of [15, 16] was used to study a supersonic ($M_\infty = 5$) flow of a sharp-nose circular cone with a half-angle $\theta_c = 4°$ and isothermal surface ($T_{w0} = T_w/T_0 = 0.5$, where T_w and T_0 denote the temperature of the surface subjected to flow and the stagnation temperature of unperturbed flow, respectively). A cone of finite length L was treated; this length was taken to be the characteristic linear dimension. The outlet boundary of the computational domain was located on the sharp edge of the bottom section, so that the flow in the near wake behind the cone was not calculated. This approach to the problem corresponds to treatment of flow past a semi-infinite cone.

Assuming the symmetry of flow, the calculations were performed on a nonuniform 41×101×101 grid (in the longitudinal, normal, and circumferential directions, respectively) in the case of laminar flow past the cone and on a nonuniform 41×81×71 grid in the case of laminar-turbulent flow.

Two series of calculations were performed. In the first series, the effect of the angle of attack ($0° \le \alpha \le 15°$) was investigated for the Reynolds numbers $\mathrm{Re} = \rho_\infty V_\infty L/\mu_\infty = 10^5$ (laminar flow) and $\mathrm{Re} = 10^7$ (laminar-turbulent flow). In the second series of calculations, the effect of the Reynolds number ($10^4 \le \mathrm{Re} \le 10^8$) at an angle of attack $\alpha = 8°$ was investigated. In so doing, numerical simulation of flow past a thin cone involved the use of Navier–Stokes equations for numbers $10^4 \le \mathrm{Re} \le 10^6$ and of Reynolds equations for numbers $10^6 \le \mathrm{Re} \le 10^8$.

THE STRUCTURE OF FLOW FIELD

The effect of the determining parameters of the problem on the structure of flow field in the vicinity of the thin cone may be judged by the pattern of limiting lines of flow on the surface subjected to flow. The effect of the angle of attack for laminar flow ($\mathrm{Re} = 10^5$) is shown in Fig. 1 and that for laminar-turbulent flow ($\mathrm{Re} = 10^7$) past the cone – in Fig. 2, and the effect of the Reynolds number at a fixed angle of attack ($\alpha = 8°$) is shown in Fig. 3.

The Effect of the Angle of Attack

At zero angle of attack, the flow of gas in the vicinity of the cone is axisymmetric, and the limiting lines of flow are straight lines issuing from the sharp vertex of the body (Figs. 1a and 2a).

One and the same flow pattern is observed on the windward side of the cone for all treated angles of attack: the line of spreading is located on the cone surface in the plane of symmetry, and the gas flows from the windward side to the leeward side. The structure of flow field on the leeward side depends strongly on the angle of attack and Reynolds number; in so doing, the gas flow is non-separation flow at angles of attack $\alpha < 4°$ and separation flow at $\alpha \ge 4°$. In view of this, the development of the structure of flow field on only the leeward side of the cone is treated below.

At small angles of attack ($\alpha < 4°$), the flow past the cone is non-separation flow, and the line of runoff is located in the plane of symmetry on the leeward side. At $\alpha = 4°$, a transverse separation of flow is initiated in the neighborhood of the symmetry plane, which is so insignificant that it is unnoticed in the patterns of limiting lines of flow which are close to the respective patterns at small angles of attack (Figs. 1b and 2b).

A developed region of transverse separation flow is observed at moderate and large angles of attack ($\alpha > 4°$) on the leeward side of the cone for both values of the Reynolds number. The patterns of limiting lines of flow indicate that the flow remains non-separation in some neighborhood of the sharp vertex of the body, and it is only at some distance downstream of the vertex that a transverse separation is formed. The size of the separation zone increases with the angle of attack, and its beginning shifts upstream somewhat. The development of the structure of separation flow is seriously affected by the Reynolds number.

In the case of laminar flow ($\mathrm{Re} = 10^5$), the structure of the separation zone on the leeward side has one and the same form for all angles of attack: the classical flow pattern according to two-vortex scheme is realized in its every cross section. An increase in the angle of attack causes qualitative changes in the characteristics of the separation zone.

In the case of laminar-turbulent flow past the cone ($\mathrm{Re} = 10^7$), a complex evolution of the separation zone structure is observed as a function of the angle of attack (Fig.2). At $\alpha = 4°$ (as was observed above),

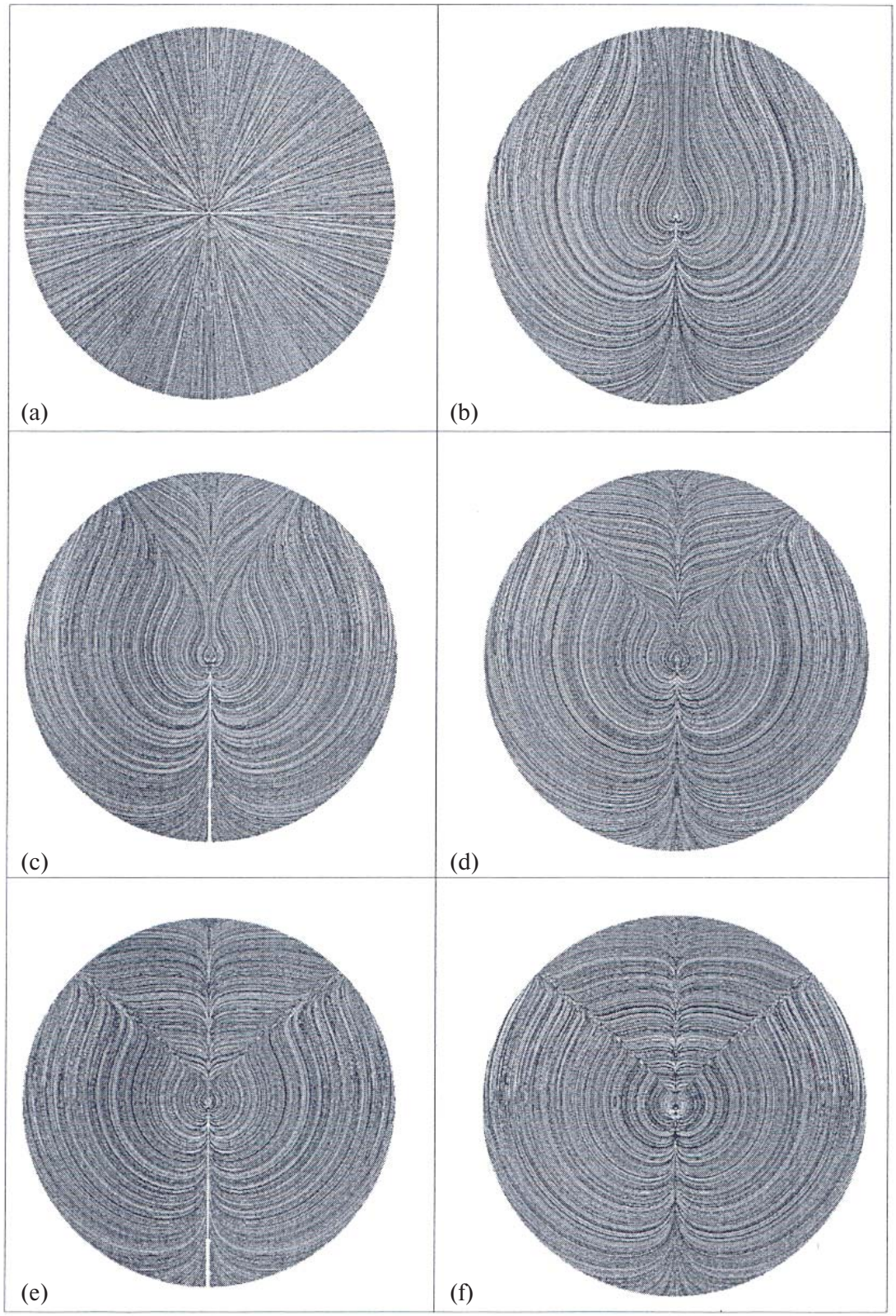

Fig. 1. The patterns of limiting lines of flow on the surface of a sharp-nose circular isothermal (T_{w0} = 0.5) cone at M_∞ = 5 and Re = 10^5 (front view, laminar flow): (a) α = 0°, (b) α = 4°, (c) α = 6°, (d) α = 8°, (e) α = 10°, (f) α = 15°.

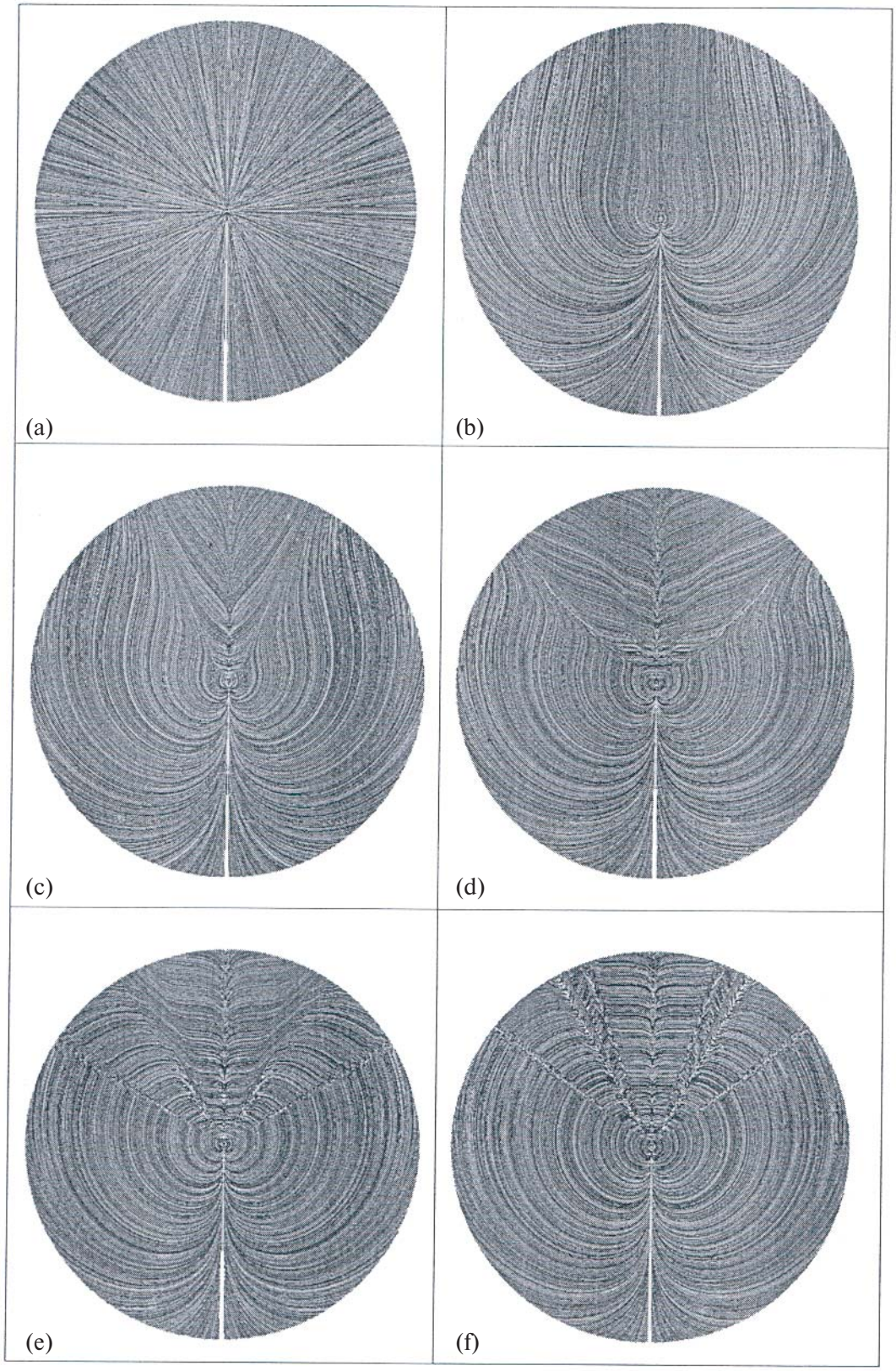

Fig. 2. The patterns of limiting lines of flow on the surface of a sharp-nose circular isothermal (T_{w0} = 0.5) cone at M_∞ = 5 and Re = 10^7 (front view, laminar-turbulent flow): (a) α = 0°, (b) α = 4°, (c) α = 6°, (d) α = 8°, (e) α = 10°, (f) α = 15°.

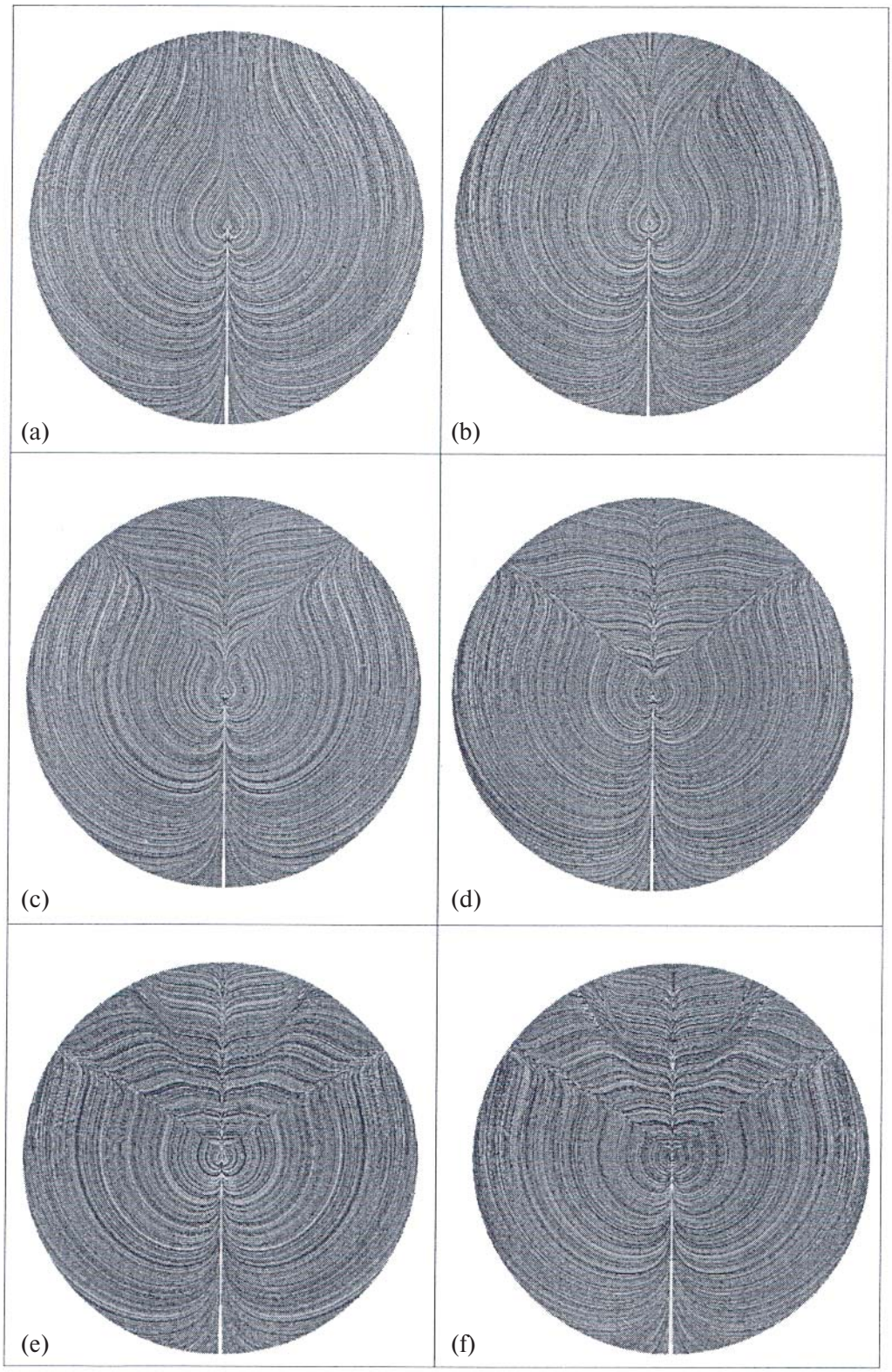

Fig. 3. The patterns of limiting lines of flow on the surface of a sharp-nose circular cone with an isothermal surface (T_{w0} = 0.5) at M_∞ = 5 and angle of attack α = 8° (front view): (a) Re = 10^4, (b) Re = 3×10^4, (c) Re = 10^5, (d) Re = 3×10^5, (e) Re = 10^6, (f) Re = 10^6 (laminar-turbulent flow), (g) Re = 3×10^6, (h) Re = 10^7, (i) Re = 3×10^7, (j) Re = 10^8.

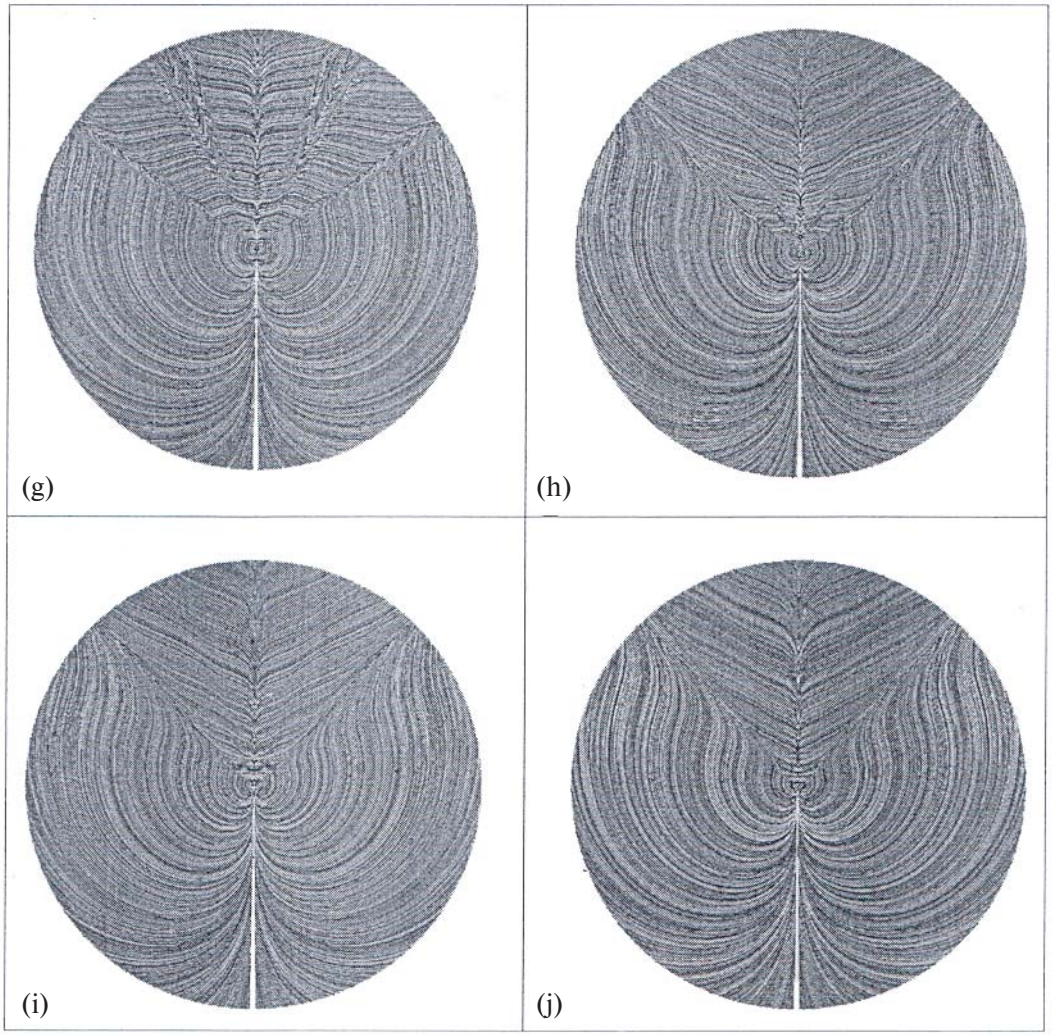

Fig. 3. End.

conditions for transverse separation of flow are developed on the leeward side of the cone (Fig. 2b). At $\alpha =$ $= 6°$, a separation zone with transverse flow and two vortexes of opposite rotation is formed in accordance with the classical scheme (Fig. 2c). At the angle of attack $\alpha = 8°$ (Fig. 2d), a secondary transverse separation and attachment of flow occur within the separation zone in its small initial region. With further increase of the angle of attack, the extent of the region of secondary separation and attachment of flow increases (Fig. 2e) and, at the angle of attack $\alpha = 15°$ (Fig. 2f), it propagates along the entire leeward side of the cone.

The foregoing data are indicative of the significant effect of the Reynolds number on the structure and characteristics of the separation zone on the leeward side of a thin cone. This effect was studied in more detail for the angle of attack $\alpha = 8°$, in the case of which a developed zone of separation flow forms on the leeward side for large values of the Reynolds number.

The Effect of the Reynolds Number

At $\mathrm{Re} = 10^4$ (Fig. 3a), the flow past the leeward side of the cone occurs without separation, and it is only in the stern part that conditions for transverse separation of flow are developed. At $\mathrm{Re} = 3\times10^4$ (Fig. 3b), transverse separation and attachment of flow is observed in the stern part of the body; with a subsequent increase in Re, the size of the separation zone increases, but the structure of separation flow remains qualitatively unvaried (Figs. 3c and 3d). At $\mathrm{Re} = 10^6$ (Figs. 3e and 3f), qualitative changes occur in the structure of separation flow: secondary separation and attachment of flow arise in the stern part of

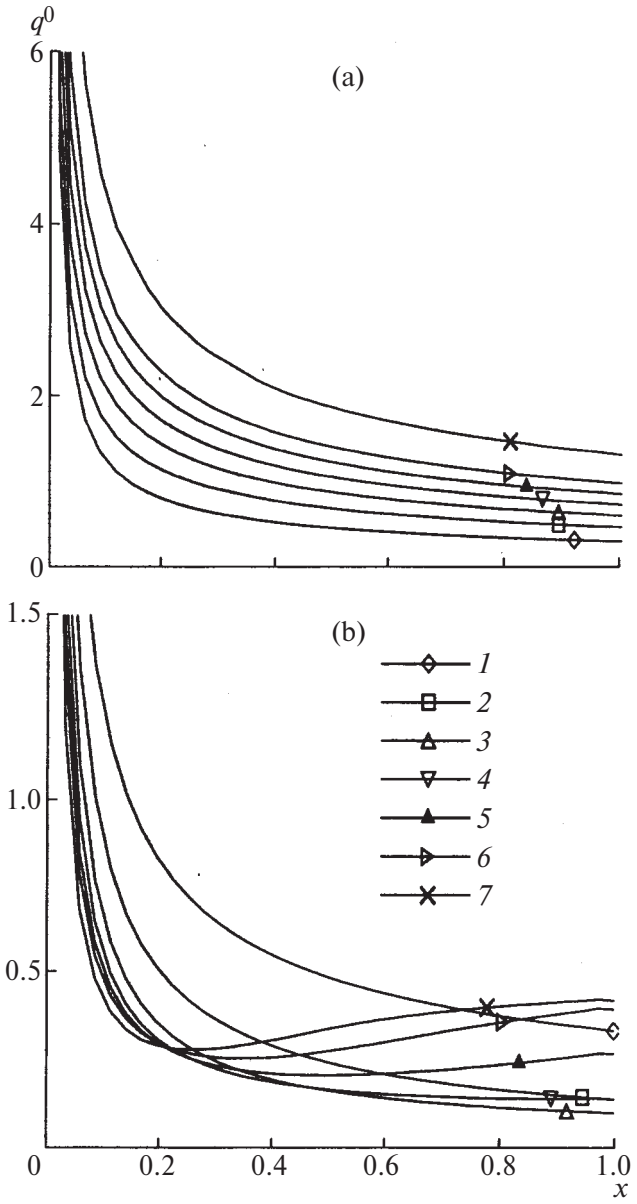

Fig. 4. The effect of the angle of attack on the distribution $q^0 = q_w\sqrt{\mathrm{Re}}$ in the symmetry plane of a sharp-nose circular cone with an isothermal surface ($T_{w0} = 0.5$) at $M_\infty = 5$ and $\mathrm{Re} = 10^5$ (laminar flow): (a) windward side, (b) leeward side; (*1*) $\alpha = 0°$, (*2*) $\alpha = 2°$, (*3*) $\alpha = 4°$, (*4*) $\alpha = 6°$, (*5*) $\alpha = 8°$, (*6*) $\alpha = 10°$, (*7*) $\alpha = 15°$.

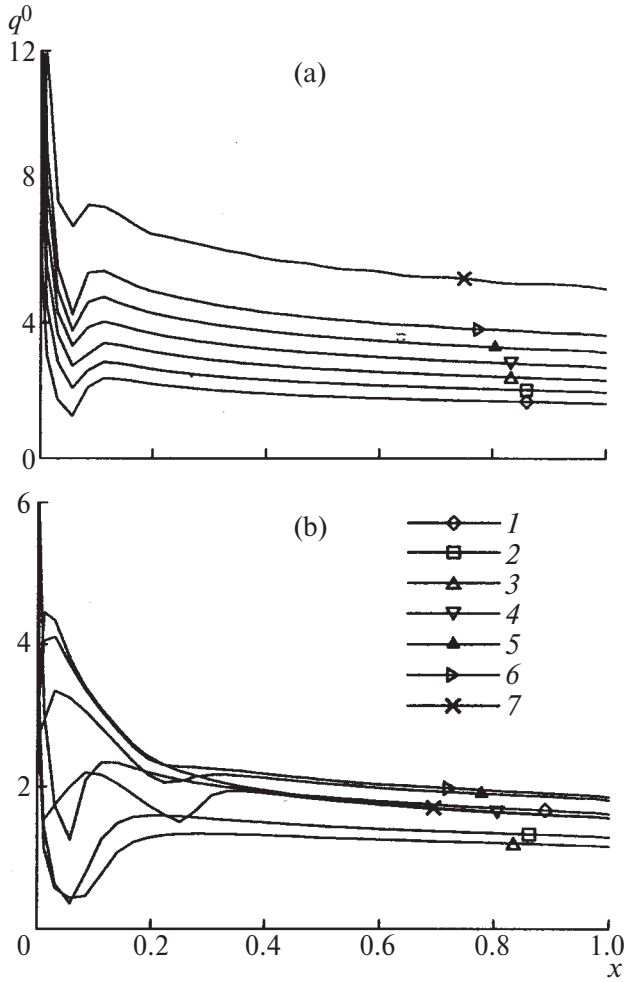

Fig. 5. The effect of the angle of attack on the distribution $q^0 = q_w\sqrt{\mathrm{Re}}$ in the symmetry plane of a sharp-nose circular cone with an isothermal surface ($T_{w0} = 0.5$) at $M_\infty = 5$ and $\mathrm{Re} = 10^7$ (laminar-turbulent flow): (a) windward side, (b) leeward side; (*1*) to (*7*) as in Fig. 4.

the separation zone. Note that, with this value of the Reynolds number, the calculations were performed using both Navier–Stokes and Reynolds equations. The calculation results almost coincide (cf., Figs. 3e and 3f), which points to the absence of turbulization of flow in the flow field being treated. At $\mathrm{Re} = 3\times10^6$ (Fig. 3g), the zone of separation flow increases, and tertiary separation and attachment of flow are formed in this zone. Such a complication of the structure of separation flow with increasing Reynolds number is typical of the laminar mode of flow. At $\mathrm{Re} = 10^7$ (Fig. 3h), the structure of flow in the separation zone is simplified compared to the previous case: the tertiary separation and attachment of flow disappear completely, and the region of secondary separation and attachment of flow is reduced significantly and located in the initial portion of the separation zone. In addition, a significant reduction of the size of the separation zone is observed. All this points to the turbulization of flow in the stern part of the cone. With a further increase in the Reynolds number (Figs. 3i and 3j),

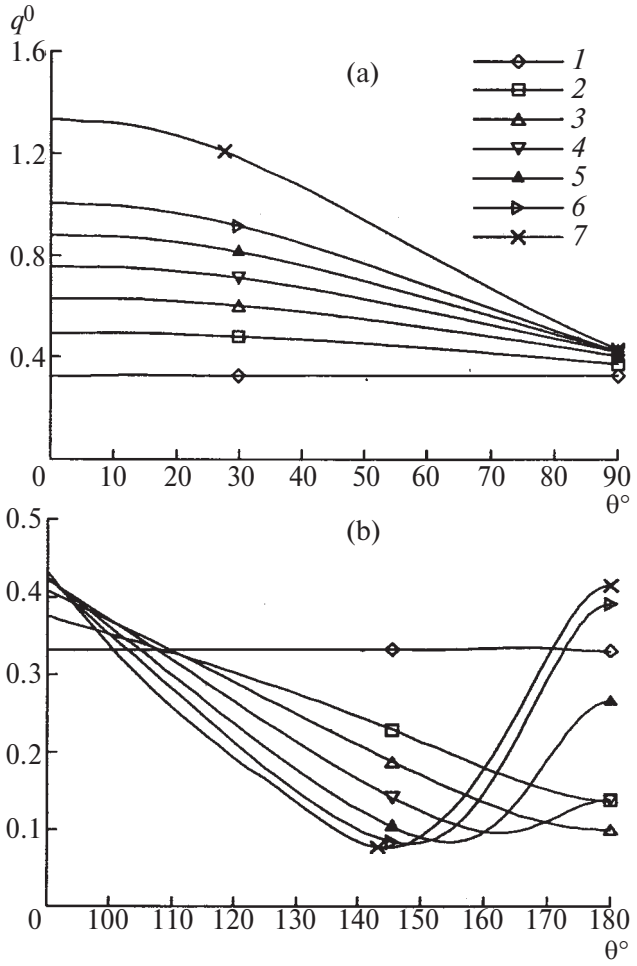

Fig. 6. The effect of the angle of attack on the distribution $q^0 = q_w\sqrt{\mathrm{Re}}$ in the cross section (x = = 1) of a sharp-nose circular cone with an isothermal surface (T_{w0} = 0.5) at M_∞ = 5 and Re = 10^5 (laminar flow): (a) windward side, (b) leeward side; (*1*) to (*7*) as in Fig. 4.

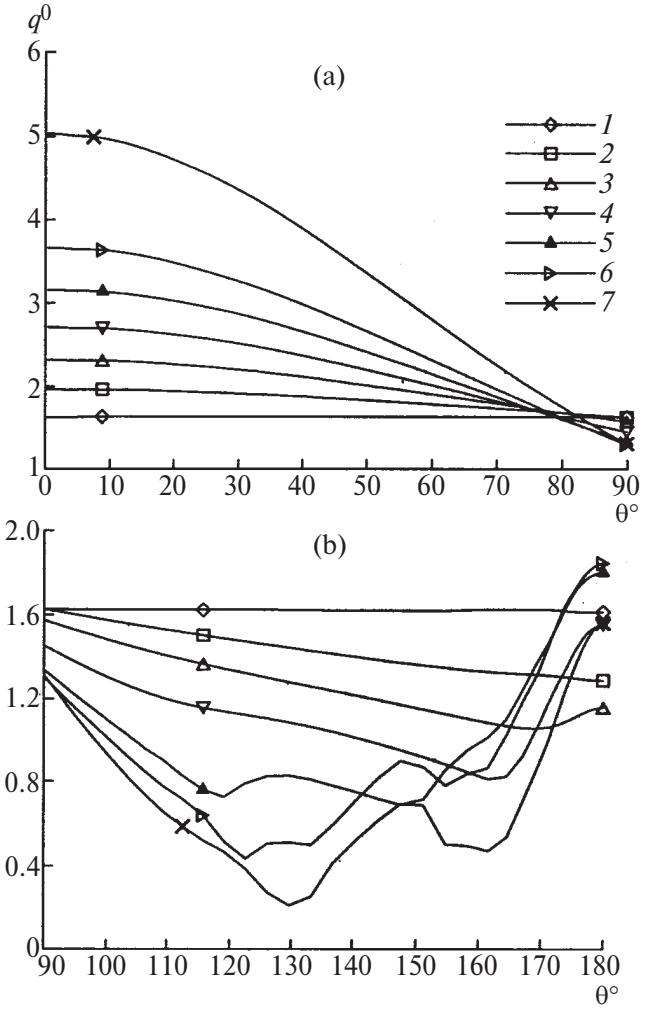

Fig. 7. The effect of the angle of attack on the distribution $q^0 = q_w\sqrt{\mathrm{Re}}$ in the cross section (x = = 1) of a sharp-nose circular cone with an isothermal surface (T_{w0} = 0.5) at M_∞ = 5 and Re = 10^7 (laminar-turbulent flow): (a) windward side, (b) leeward side; (*1*) to (*7*) as in Fig. 4.

the secondary separation and attachment of flow disappear completely and a decrease in the size of the separation zone is observed, which is indicative of the expansion of the region of turbulent flow.

AERODYNAMIC HEATING

In analyzing the problem within the framework of the theory of laminar boundary layer, the dependence of the solution on the Reynolds number shows up explicitly; in particular, the local aerodynamic characteristics vary inversely with the square root of the Reynolds number. Because we treat the flow past a sharp cone at high values of the Reynolds number, the results of calculations of heat transfer are represented as the dependence of the dimensionless quantity $q^0 = q_w\sqrt{\mathrm{Re}}$ on one or other independent variable associated with the surface subjected to flow. Here, $q_w^* = \rho_\infty V_\infty H_\infty q_w$ is the local heat flux, and H_∞ is the total enthalpy of unperturbed flow. For laminar-turbulent flow past the cone, the calculation results are given in the same form as for laminar flow for the purpose of identifying the regions of transition and turbulent flow. Note that the results given below make it possible to judge the behavior of heat transfer coefficient as a function of the determining parameters of the problem; however, because of approximate validity of the Reynolds analogy, the inferences will

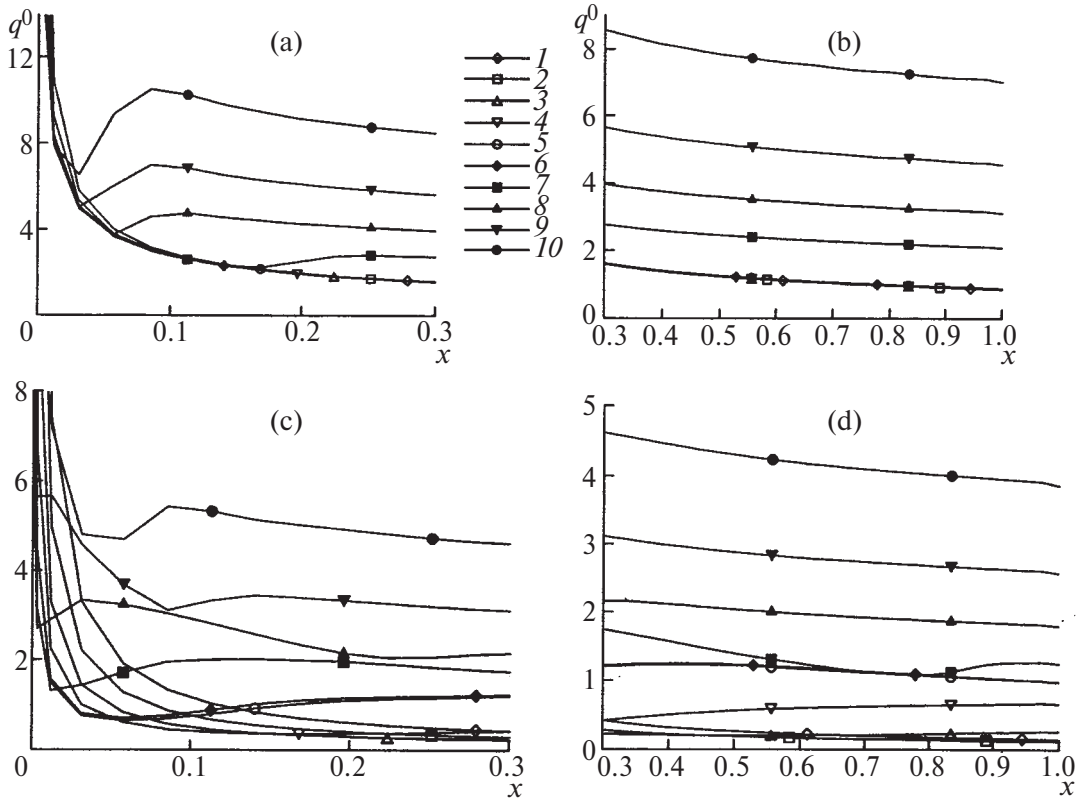

Fig. 8. The effect of the Reynolds number on the distribution $q^0 = q_w\sqrt{\mathrm{Re}}$ in the symmetry plane of a sharp-nose circular cone with an isothermal surface ($T_{w0} = 0.5$) at $M_\infty = 5$ and angle of attack $\alpha = 8°$: (a, b) windward side, (c, d) leeward side; (*1*) $\mathrm{Re} = 10^4$, (*2*) $\mathrm{Re} = 3\times10^4$, (*3*) $\mathrm{Re} = 10^5$, (*4*) $\mathrm{Re} = 3\times10^5$, (*5*) $\mathrm{Re} = 10^6$, (*6*) $\mathrm{Re} = 10^6$, (*7*) $\mathrm{Re} = 3\times10^6$, (*8*) $\mathrm{Re} = 10^7$, (*9*) $\mathrm{Re} = 3\times10^7$, (*10*) $\mathrm{Re} = 10^8$; (*1–5*) laminar flow, (*6–10*) laminar-turbulent flow.

relate qualitatively to the longitudinal (radial) component of local friction drag as well.

As was mentioned above, the line of spreading is located on the windward side in the symmetry plane of the sharp cone at all angles of attack. On this line, the local values of heat flux (Fig. 4a) under conditions of laminar flow past a body ($\mathrm{Re} = 10^5$) decrease monotonically in the longitudinal direction at $\alpha = \mathrm{const}$ and increase monotonically with increasing angle of attack at $x = \mathrm{const}$. Here, $x^* = xL$ is the coordinate directed along the cone axis and reckoned from its vertex downstream. The line of runoff is located on the leeward side of the cone in the flow symmetry plane at small angles of attack; in the case of moderate and large angles of attack, this line is replaced by the line of spreading as the transverse separation and attachment of flow is initiated and develops. Therefore, the local heat fluxes in the cross section of the cone being treated (Fig. 4b) vary nonmonotonically both in the longitudinal direction and as a function of the angle of attack. The nonmonotonicity of variation of the heat flux in the longitudinal direction at $\alpha = \mathrm{const}$ is observed for high values of the angle of attack and leads to the emergence of a local minimum located in the neighborhood of the point of initiation of transverse separation. As a result of nonmonotonicity of variation as a function of the angle of attack, the values of local heat fluxes in the cross section of the body on the leeward side become commensurable with their values on the windward side.

Analogous calculation results for laminar-turbulent flow past the cone ($\mathrm{Re} = 10^7$) are given in Fig. 5. According to these data, a laminar-turbulent transition for the numbers Re and M_∞ being treated is observed in the neighborhood of the sharp vertex on both the windward and leeward sides, so that the flow of gas in the boundary layer on the larger part of the cone surface subjected to flow is turbulent. The presence of laminar-turbulent transition defines a higher degree of nonmonotonicity of variation of local heat fluxes in

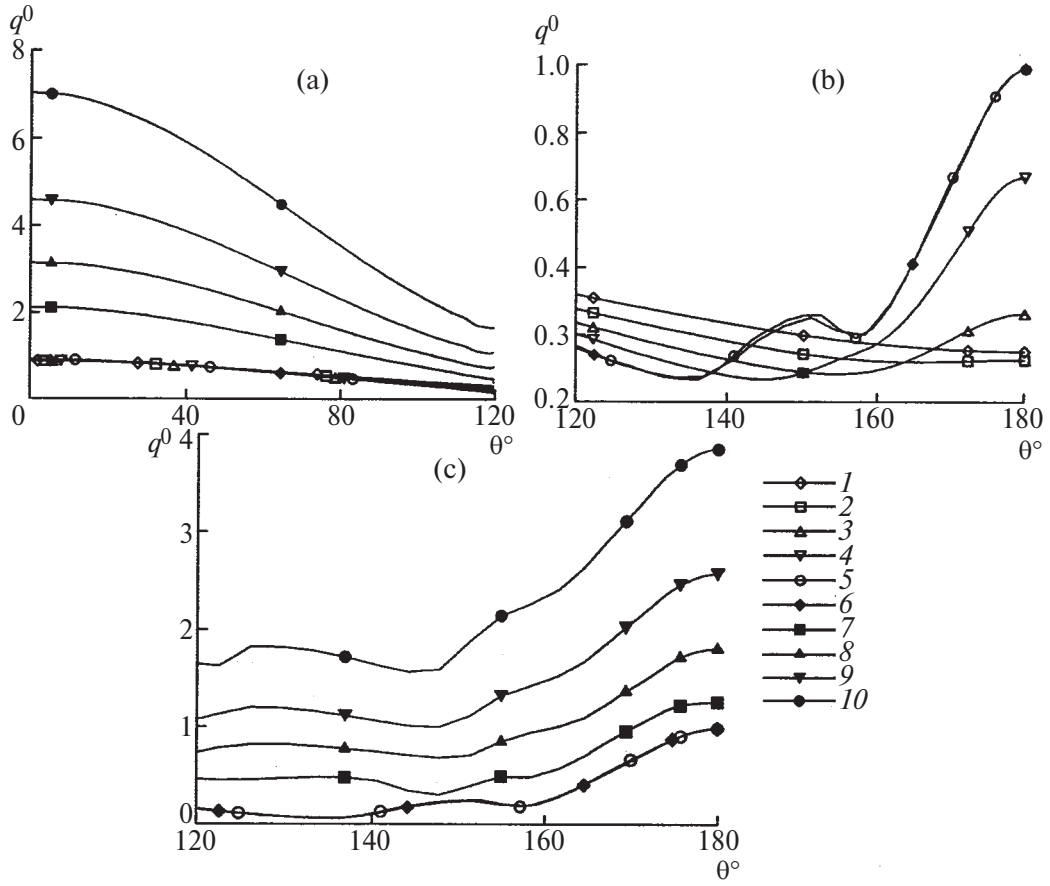

Fig. 9. The effect of the Reynolds number on the distribution $q^0 = q_w\sqrt{\mathrm{Re}}$ in the cross section (x = 1) of a sharp-nose circular cone with an isothermal surface (T_{w0} = 0.5) at M_∞ = 5 and angle of attack α = 8°: (a) windward side, (b, c) leeward side; (*1*) to (*10*) as in Fig. 8.

the symmetry plane of flow compared to the case of laminar flow past the cone.

We will analyze the effect of the angle of attack on the distribution of heat flux in the cross section of the cone. For this purpose, we will restrict ourselves to treating the bottom cross section (x = 1), for which the results of calculation for the case of laminar flow are given in Fig. 6 and the results for the case of laminar-turbulent flow – in Fig. 7. Here, θ is the central angle reckoned from the plane of symmetry on the windward side of the body.

In the case of laminar flow past the cone (Fig. 6) at small angles of attack ($0° < \alpha \le 4°$), the heat flux decreases monotonically during transition from the windward to leeward side and, in the plane of symmetry, assumes the maximal value on the windward side and the minimal value on the leeward side. In the case of moderate and large values of the angle of attack ($\alpha > 4°$), the heat flux varies nonmonotonically during transition from the windward to leeward side because of the presence of transverse separation and assumes local maximal values in symmetry plane of the body and a local minimal value on the leeward side in the neighborhood of the point of transverse separation. The smooth variation of heat flux in the separation zone is indicative of the simple structure of flow in the separation zone.

The heat flux behavior in the bottom cross section in the case of laminar-turbulent flow past the cone (Fig. 7) is largely similar; however, some differences are observed caused by the structure of flow in the separation zone. During transition from the windward to leeward side, the heat flux at small angles of attack ($0° < \alpha < 4°$) decreases monotonically exhibiting extrema in the symmetry plane and, at moderate and large angles of attack ($\alpha \ge 4°$), it varies nonmonotonically exhibiting a number of local extrema. The presence of several extrema in the separation zone is indicative of the complex structure of flow in this zone.

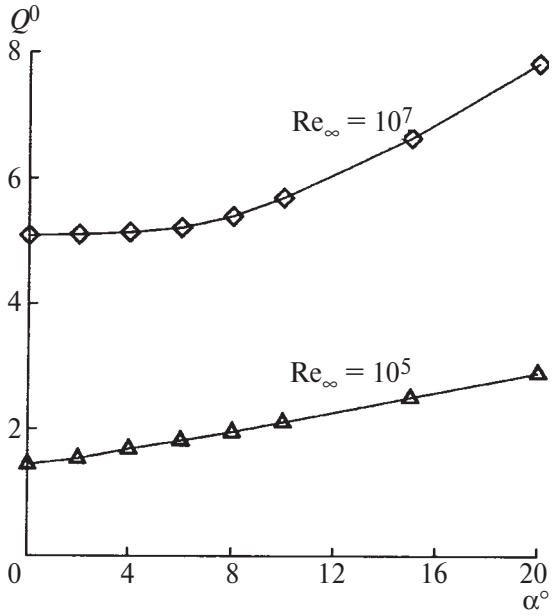

Fig. 10. The effect of the angle of attack on $Q^0 = Q_w\sqrt{\mathrm{Re}}$ of a sharp-nose circular isothermal (T_{w0} = 0.5) cone at M_∞ = 5 and a fixed value of Re.

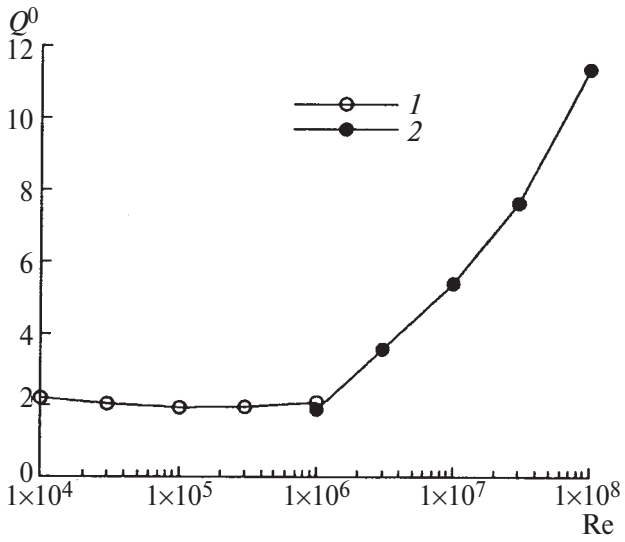

Fig. 11. The effect of the Reynolds number on $Q^0 = Q_w\sqrt{\mathrm{Re}}$ of a sharp-nose circular isothermal (T_{w0} = 0.5) cone at M_∞ = 5 and angle of attack α = 8°: (*1*) results of calculations using Navier–Stokes equations, (*2*) Reynolds equations.

The effect of the Reynolds number on the local aerodynamic characteristics of a sharp cone was investigated in detail for the angle of attack α = 8°. The results of calculations of local values of heat flux are given in Figs. 8 and 9. According to these data, it was for the first time that a laminar-turbulent transition was observed on the cone surface subjected to flow at $10^6 < \mathrm{Re} < 3\times10^6$; with further increase in the Reynolds number, the point of transition shifts upstream, which fact defines the increase in the heat fluxes and the simplification of the structure of flow field on the leeward side of the body.

The variation of the Reynolds number does not affect the overall structure of flow field on the windward side of the cone. As a result, on the windward side of the body the results of calculation of q^0 for different values of Re in the case of laminar flow fit a unified dependence curve (Figs. 8a, 8b, and 9a), and the prediction data corresponding to turbulent flow in the boundary layer deviate from this dependence curve and indicate the position of the transition point and the degree of increase in the local heat flux due to turbulization of flow.

On the leeward side of the cone, the variation of the Reynolds number has a significant effect on the overall structure of flow field; therefore, the distribution of q^0 in both the symmetry plane and cross section of the body is more complex compared to that on the windward side (Figs. 8c, 8d, 9b, and 9c).

Of certain applied interest is the total heat flux delivered from the cone surface subjected to flow into a flying vehicle. Therefore, the known distribution of local heat flux along the surface subjected to flow was used to calculate its total value. The results of these calculations, which demonstrate the effect of Re and angle of attack on the overall heat flux, are given in Figs. 10 and 11.

CONCLUSIONS

The aerodynamic heating of a thin sharp-nose circular cone with a half-angle $\theta_c = 4°$ in a supersonic flow (M_∞ = 5) of perfect gas was investigated for low, moderate, and high values of angle of attack. The calculations on the assumption of flow symmetry were performed using Navier–Stokes equations for Reynolds number values of $10^4 \le \mathrm{Re} \le 10^6$ and Reynolds equations for Reynolds number values of $10^6 \le \mathrm{Re} \le 10^8$. In the absence of transverse separation, the local heat flux in the cone cross section decreases monotonically during transition from the windward to leeward side exhibiting extreme values in the symmetry plane, namely, a maximum on the windward side and a minimum on the leeward side. The presence of transverse separation

causes a qualitative variation of the distribution of heat flux in the cross section of the body. This distribution becomes nonmonotonic, exhibiting local maxima in the symmetry plane and a local minimum in the neighborhood of the point of transverse separation; depending on the structure of flow in the separation zone, additional extrema of heat flux may arise on the leeward side. As regards aerodynamic heating, note that in the majority of cases the absolute maximum of heat flux in the cone cross section is observed on the windward side of the cone; however, at high values of the Reynolds number and attack angle, the local maximum on the leeward side comes to be of the same order of magnitude as its value on the windward side.

ACKNOWLEDGMENTS

This study was supported by the grant of the President of the Russian Federation for support of leading scientific schools (NSh-2001-2003.1).

REFERENCES

1. Bashkin, V.A., *Treugol'nye kryl'ya v giperzvukovom potoke* (Delta Wings in Hypersonic Flow), Moscow: Mashinostroenie, 1984.
2. Bashkin, V.A. and Dudin, G.N., *Prostranstvennye giperzvukovye techeniya vyazkogo gaza* (Three-Dimensional Hypersonic Flows of Viscous Gas), Moscow: Nauka, Fizmatlit, 2000.
3. Jorgensen, L.H., Elliptic Cones alone and with Wings at Supersonic Speeds, *Report 1376–NASA*, 1957.
4. Peake, D.J., Owen, F.K., and Higuchi, H., Symmetric and Asymmetric Separations about a Yawed Cone, in *High Angle of Attack Aerodynamics, AGARD-CP-247*, 1978, p. 16-1.
5. Krasil'shchikov, A.P. and Nosov, V.V., Some Characteristic Features of Aerodynamic Characteristics of Cones in a Viscous Hypersonic Flow, in *Aeromekhanika* (Aeromechanics), Moscow: Nauka, 1976, p. 199.
6. McRae, D.S. and Hussaini, M.Y., Numerical Simulation of Supersonic Cone Flow at High Angle of Attack, in *High Angle of Attack Aerodynamics, AGARD-CP-247*, 1978, p. 23-1.
7. Beam, R. and Warning, R.F., *AIAA J.*, 1978, vol. 16, p. 393.
8. Steger, J.L., *AIAA J.*, 1978, vol. 16, p. 679.
9. Hollanders, H. and Devezeaux de Lavergne, D., High Speed Laminar Near Wake Flow Calculations by an Implicit Navier-Stokes Solver, *AIAA Paper 87-1157*, 1987.
10. Egorov, I.V. and Zaitsev, O.L., *Zh. Vychisl. Mat. Mat. Fiz.*, 1991, vol. 31, no. 2, p. 286.
11. Bashkin, V.A., Egorov, I.V., and Egorova, M.V., *Izv. Ross. Akad. Nauk Mekh. Zhidk. Gaza*, 1993, no. 6, p. 107.
12. Bashkin, V.A., Egorov, I.V., Egorova, M.V., and Ivanov, D.V., *Izv. Ross. Akad. Nauk Mekh. Zhidk. Gaza*, 2000, no. 5, p. 31.
13. Coakley, T.J. and Huang, P.G., Turbulence Modeling for High Speed Flows, *AIAA Paper 92-0436*, 1993.
14. Bashkin, V.A., Egorov, I.V., and Ivanov, D.V., *Izv. Ross. Akad. Nauk Mekh. Zhidk. Gaza*, 1998, no. 2, p. 143.
15. Bashkin, V.A., Egorov, I.V., Ivanov, D.V., and Pafnut'ev, V.V., *Zh. Vychisl. Mat. Mat. Fiz.*, 2002, vol. 42, no. 12, p. 1864.
16. Bashkin, V.A., Egorov, I.V., Ivanov, D.V., and Plyashechnik, V.I., *Izv. Ross. Akad. Nauk Mekh. Zhidk. Gaza*, 2003, no. 1, p. 123.
17. Chen, Yu.Yu., *Raketn. Tekh. Kosmonavt.*, 1969, vol. 7, no. 10, p. 255 (Russ. transl. of *AIAA J.*).